Experimental study of steady and unsteady free surface flows with water-clay mixtures

Étude expérimentale d'écoulements à surface libre permanents et non permanents d'eau très chargée en argile

D. KOMATINA, M. JOVANOVIĆ, *University of Belgrade, Faculty of Civil Engineering, 11000 Belgrade, POBox 805, Yugoslavia, E-mail: DKOMAT@irc.grf.bg.ac.yu*

SUMMARY
The steady and unsteady free-surface flow of hyperconcentrated water-kaolinite clay mixtures is analysed experimentally. These mixtures exhibit non-Newtonian behaviour if volumetric concentrations of solid particles exceed about 10%. The viscosity-concentration correlations, determined by rotary viscometer, indicate that the Bingham model can be used to describe such fluids. Using the rheological parameters of this model, the water-clay laminar flow friction factors can be determined either by calculating the Reynolds and Hedström numbers, or by applying the concept of the extended Reynolds number. A quantitative analysis of the unsteady dam-break type of the free-surface flow is presented, giving a comparison of flow depth profiles and propagation rates between the investigated mixtures and water.

RÉSUMÉ
L'article présente l'étude expérimentale de l'écoulement permanent et nonpermanent à surface libre de mélanges hyperconcentrés d'eau et d'argile kaolinite. Ces mélanges se comportent d'une façon non-newtonienne, lorsque la phase solide dépasse une concentration volumétrique de 10%. Les corrélations entre la viscosité et la concentration, déterminés par un viscosimètre rotatif, ont indiqué que le modèle de Bingham décrit bien les mélanges considérés. En utilisant les paramètres rhéologiques de ce modèle, les coefficients de perte de charge en régime laminaire, peuvent être déterminés par les nombres de Reynolds et Hedström, ou suivant le concept d'un nombre de Reynolds étendu. Une analyse quantitative de l'écoulement non-permanent du type onde de submersion de barrage est présenté, avec une comparaison des profondeurs et des vitesses de propagation d'ondes des mélanges étudiés et de l'eau pure

1 Introduction

Hyperconcentrated water-clay mixtures exhibit non-Newtonian behaviour, and in order to describe the flow characteristics of such fluids, rheological relationships need to be established. In this paper such a relationship is presented for water-kaolinite clay mixtures in terms of volumetric concentration of the solid phase. Several authors have concluded that fluids with solid concentrations above 10% can be considered non-Newtonian [1], [12]. Their rheological properties, within a considerable range of shear rates, can be described by the Herschel-Bulkley model [1], while for shear rates occurring in most of the free-surface flows, the simpler Bingham model may be used [5], [6], [9], [15]. At extremely low shear rates, the pseudoplastic model has been suggested [9].
The parameters of the Bingham model - the yield stress and the plastic viscosity, determined by laboratory measurements, can be used to calculate the friction coefficient for the laminar flow. The results of such laboratory measurements are presented, and the friction factor relations for water-kaolinite mixtures are given in terms of the standard and the extended Reynolds numbers, following the approach of some previous researchers [9], [13]. The experimental study has been extended to the unsteady free-surface water-clay flows. Results of such investigations (to the authors' knowledge scarce in literature), are very important for understanding and predicting the hyperconcentrated river

Revision received April 23, 1997. Open for discussion till April 30, 1998.

flows and dam-break phenomena. The experimental results, showing the dependence of the unsteady flow parameters on the concentration of the solid phase, are presented. This investigation has provided a solid experimental data base valuable for development of non Newtonian flow numerical models.

2 Rheological characteristics of investigated fluids

The considered fluids are water-kaolinite clay mixtures with different concentration of the solid particles. The mean diameter of particles is 0.006 mm. The specific density of the clay material is 2.65, and its chemical composition: SiO_2 (≈50%), Al_2O_3 (37%), CaO (<5%) and Fe_2O_3 (<3%). Nine liquid-solid mixtures were investigated, whose density (ζ_m) is expressed in terms of concentration (by volume C_v, and by weight C_w) in Table 1.

Table 1. Density of investigated mixtures

C_v (%)	2.0	4.0	6.2	8.6	11.2	13.9	16.9	20.1	23.6
C_w (%)	5	10	15	20	25	30	35	40	45
ρ_m (kg/m^3)	1032	1066	1103	1142	1184	1230	1279	1332	1389

The rheological properties have been determined by the coaxial cylinder rotary viscometer [4], and the rheological diagrams depicted in Fig.1 show the shear stress (τ_c) – shear rate ($\dot{\gamma}$) relationships.

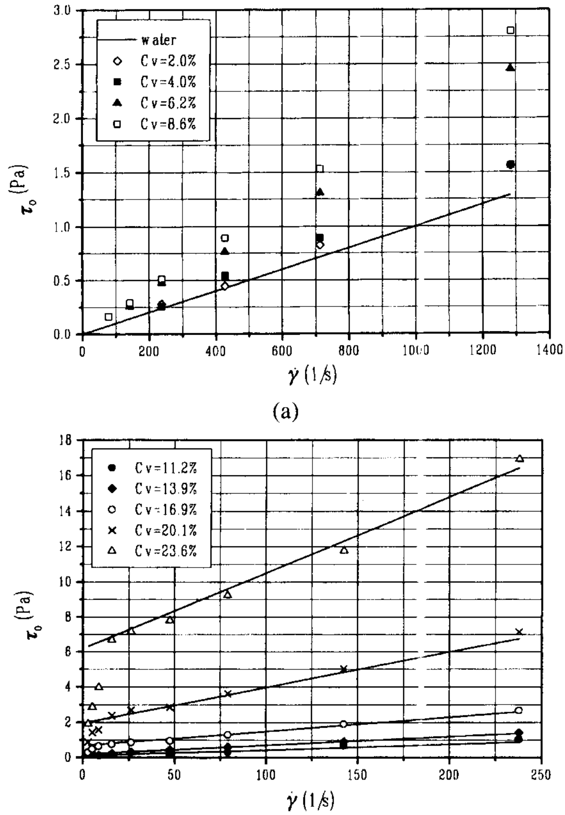

(b)

Fig. 1. Rheological relationships for water-clay mixtures: (a) volumetric concentrations up to 8.6% and (b) volumetric concentrations above 11.2%.

3 Rheological model

Considering results of the laboratory experiments, the investigated mixtures may be described by the simple Bingham model, which gives a linear relationship between the shear stress (τ) and the shear rate (du/dz)

$$\tau = \tau_c + \eta \frac{du}{dz} \tag{1}$$

where u is the local velocity, z is the vertical coordinate, and the two parameters – the yield stress τ_c, and the plastic viscosity η, are concentration dependent and are to be determined experimentally (Fig.1).

The relationships in Fig.1-(a) are linear, without an apparent yield stress. This means that the mixtures with volumetric concentrations of up to 8.6% can be considered as Newtonian fluids. This conclusion is in agreement with findings in [1] and [12]. Inspection of laboratory results pertaining to mixtures with concentrations above 11.2%, Fig.1-(b), reveals a nonlinear behaviour in the zone of small shear rates. However, these relationships can be considered predominantly linear, and if the narrow zone of nonlinearity is neglected, the Bingham model can be assumed to be valid. Dependence of the plastic viscosity (slope) and the yield stress (intercept on the ordinate) on concentration, given in Table 2 and shown in Fig.2, can be analytically defined for the given mixtures:

$$\eta = 0.621 \cdot \exp(0.173 \cdot C_v) \qquad \tau_c = 0.002 \cdot \exp(0.342 \cdot C_v) \tag{2}$$

Table 2. Parameters of the Bingham model for the investigated mixtures

Concentration C_v (%)	11.2	13.9	16.9	20.1	23.6
Yield stress τ_c (Pa)	0.10	0.20	0.69	1.96	6.19
Plastic viscosity η (mPas)	3.30	6.90	12.10	20.10	43.00

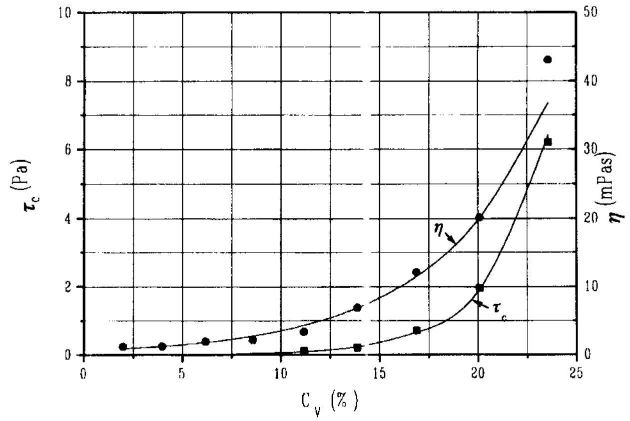

Fig. 2. Dependence of Bingham model parameters on concentration of solid particles.

4 Experimental installation

Experiments were carried out in a 4.5 m long, 0.15 m wide glass-walled laboratory flume with adjustable bottom slope (Fig.3). The steady circulation was ensured by a sludge pump. The concentration of any particular mixture was constant throughout experiments, a condition easily satisfied by the relatively small size of the experimental rig. Electrical probes, connected to a data acquisition and processing system, were used for continuous measurement of depths and velocities[1]. Digital video recordings were used for evaluation of wave characteristics in the unsteady flow experiments.

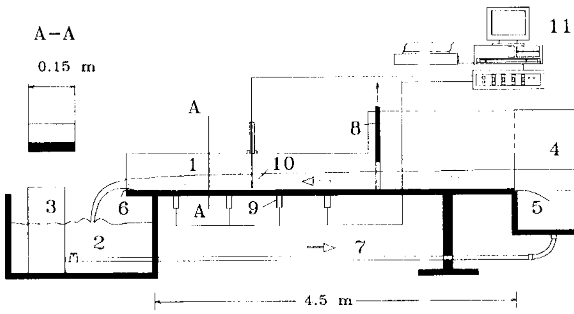

Fig. 3. Laboratory flume and measuring equipment: (1) flume; (2) lower tank; (3) pump; (4) upper tank; (5) deflector; (6) control weir; (7) fluid supply rubber tube; (8) removable gate; (9) membrane probes; (10) electromagnetic probe; (11) data acquisition and processing system.

Two types of experiments were performed. The steady flow experiments were used to determine the frictional resistance. The unsteady flow experiments were used to compare the flow characteristics of considered mixtures with those of water.

5 Steady flow analysis

Under the steady conditions, nearly uniform flow developed in the flume. The range of experimental parameters is given in Table 3. The discharge was determined volumetrically, and by velocity integration. The levels were recorded along the flume, as well as point velocities over a cross-section. The measured cross-sectional velocity distribution shown in Fig.4 can be considered uniform (in spite of relatively low values of width-to-depth ratios), indicating that effects of wall resistance are negligible.

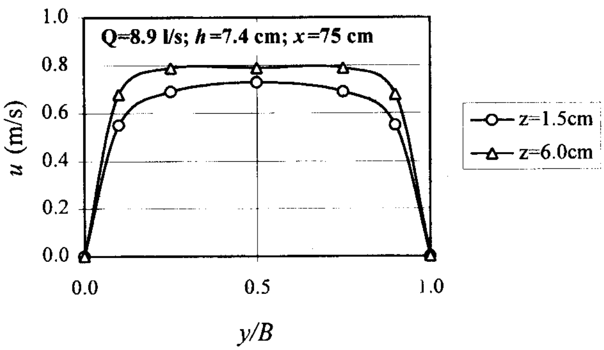

Fig. 4. Measured velocity distribution.

[1] The membrane probes "DRUCK" were used for flow depth measurement, and the electromagnetic probes UECM 200" for point velocity measurement.

The following dimensionless relation for the Darcy-Weisbach friction coefficient (*f*) was considered:

$$\Psi(f, Re_1, He) = 0 \tag{3}$$

Table 3. Range of steady-state experimental parameters

Bed slope (%)	Depth Discharge	Volumetric concentration (%)				
		0.0	4.0	8.6	13.9	20.1
0.00	h (cm)	4.3-9.4	4.0-8.3	4.3-8.2	4.5-9.5	6.5-14.7
	Q (l/s)	1.7-9.9	1.5-7.3	2.3-8.4	1.1-8.1	0.0-4.7
0.05	h (cm)	5.1-9.0	5.1-8.7	5.1-8.5	5.2-10.5	6.4-14.1
	Q (l/s)	2.4-8.9	2.2-8.5	2.9-8.7	1.4-9.3	0.3-4.7
0.10	h (cm)	3.8-8.8	3.8-8.8	3.8-8.8	4.0-10.7	5.8-13.9
	Q (l/s)	1.3-8.5	1.2-8.6	1.3-8.8	0.1-9.4	0.0-5.9

Assuming the homogeneity of mixtures, the laminar, uniform free-surface flow of the Bingham fluid can be described by the following relation [2], [9], [10], [13]:

$$\frac{3V}{h} = \frac{\tau_o}{\eta}\left[1 - \frac{3\tau_c}{2\tau_o} + \frac{1}{2}\left(\frac{\tau_c}{\tau_o}\right)^3\right] \tag{4}$$

where V, h and τ_o denote the mean cross-sectional velocity, the flow depth and the bottom shear stress respectively. The theoretical curve (4) is depicted in Fig. 5, along with experimental points for concentrations 13.9 and 20.1%, indicating a non-Newtonian character of the fluids.

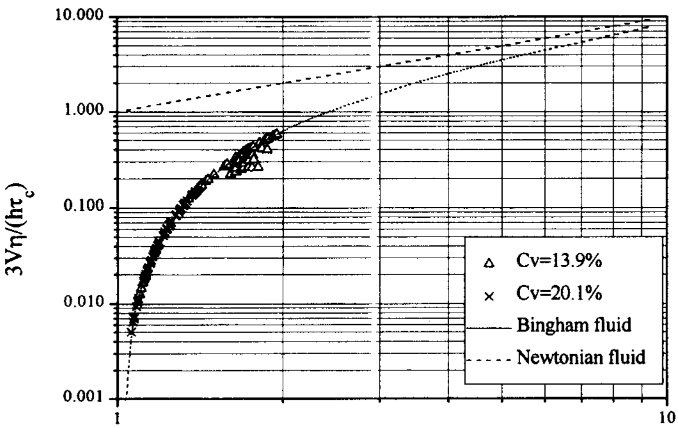

Fig. 5. Relation between the dimensionless wall shear stress and the mean velocity.

The friction coefficient can be expressed in terms of Reynolds and Hedström numbers:

$$Re_1 = \frac{\rho_m V h}{\eta} \qquad He = \frac{\tau_c \rho_m h^2}{\eta^2} \tag{5}$$

in the following way [13]:

$$\frac{1}{Re_1} = \frac{f}{6} - \frac{1}{2}\frac{He}{Re_1^2} + \frac{2}{3}\frac{He^3}{f^2 Re_1^6} \tag{6}$$

The experimentally obtained results for concentrations 13.9 and 20.1% are shown in Fig.6 (a)–(b) in addition to theoretical curves (6) (solid lines).

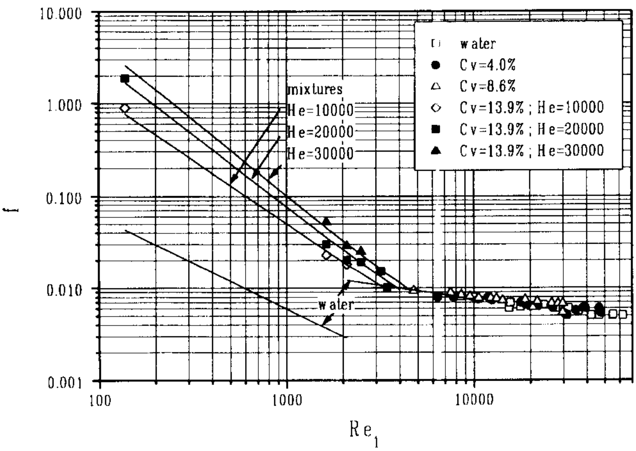

(a)

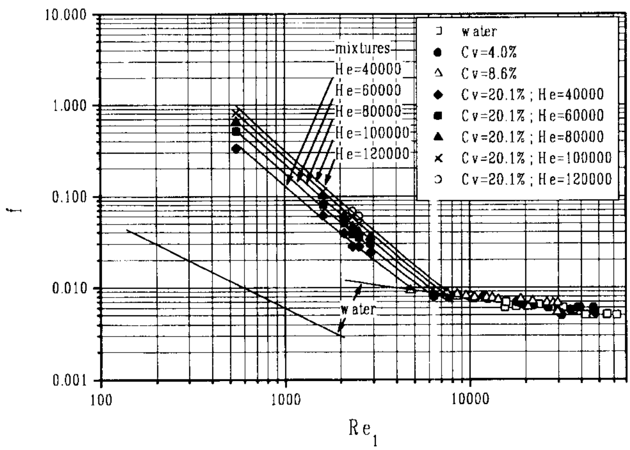

(b)

Fig. 6. Friction coefficent for laminar water-clay mixture free-surface flow in terms of Re_1 and He numbers: (a) $C_v = 13.9\%$; (b) $C_v = 20.1\%$.

If an extended Reynolds number is defined for the free-surface flow (by analogy with the pressurized Bingham flow, as described in [7], [8]):

$$Re_2 = Re_1\left[1 - \frac{3\tau_c}{2\tau_o} + \frac{1}{2}\left(\frac{\tau_c}{\tau_o}\right)^3\right] \tag{7}$$

and substituting in (4), the friction coefficient can be expressed as:

$$f = \frac{6}{Re_2} \tag{8}$$

The relation $f = f(Re_2)$ for the analysed mixtures is shown in Fig.7.

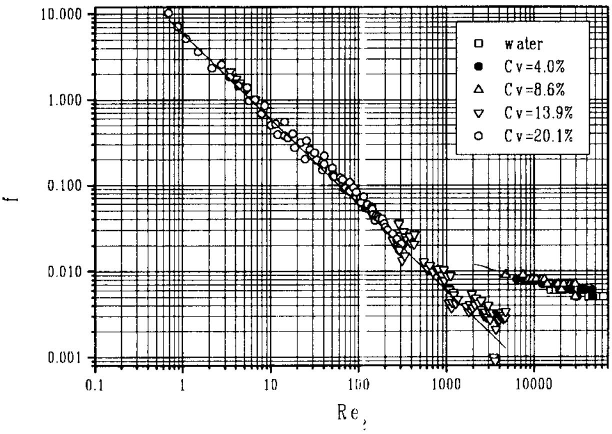

Fig. 7. Friction coefficient for laminar water-clay mixture free-surface flow in terms of the extended Reynolds number.

6 Unsteady flow analysis

A number of unsteady flow experiments were undertaken in order to investigate wave propagation characteristics of hyperconcentrated fluids. The dam-break type of flow was initiated by releasing mixtures from a reservoir situated on the upstream part of the flume (Fig.3). The release, caused by an abrupt removal of the gate between the reservoir and the channel, was practically instantaneous. The propagating positive wave was filmed by photo and video cameras. The wave celerity and the form of the wave front were determined from digitized recordings. The levels were also continuously monitored during each experiment. A total of 69 experiments were performed, with a range of initial reservoir depths of 10–30 cm, bed slopes 0.0–0.1%, and volumetric concentrations 0.0–36.1 %.

The unsteady phenomena is analysed considering the relationship between five dimensionless variables:

$$\Phi\left(\frac{x}{H}, \frac{h}{H}, S_o, t\sqrt{\frac{g}{H}}, C_v\right) = 0 \tag{9}$$

where x is distance along the channel, H- the initial reservoir depth, h-instantaneous flow depth, S_o- the channel bottom slope, t- time, and C_v- volumetric concentration.
The effect of particle concentration on the wave propagation rate is shown by a typical diagram in Fig.8, the channel slope being 0.1%. An increase of the wave front propagation time with concentration is evident. At extremely high concentrations, such as 36.1%, the wave propagates only at a small distance before reaching a "freezing point" (Fig.8).

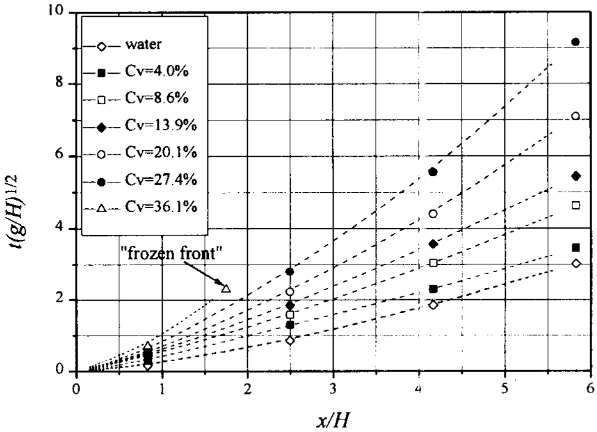

Fig. 8. Effect of particle concentration on the rate of wave front propagation.

In order to compare wave propagation velocities of mixtures and water, a ratio x_m/x_w is introduced, where subscripts m and w refer to mixture and water respectively. The values of this ratio, given in Table 4, generally decrease with concentration.

Table 4. Ratio of wave front propagation velocities.

Bed slope (%)	Initial depth (cm)	Volumetric concentration (%)					
		4.0	8.6	13.9	20.1	27.4	36.1
0.00	10	0.94	0.89	0.72	0.61	0.44	-
	20	0.76	0.72	0.60	0.48	0.34	-
	30	0.74	0.70	0.57	0.46	0.37	0.26
0.05	10	0.83	0.79	0.54	0.50	0.38	-
	20	0.81	0.63	0.52	0.42	0.31	-
	30	0.74	0.57	0.49	0.39	0.33	0.24
0.10	10	0.75	0.71	0.50	0.46	0.36	-
	20	0.70	0.57	0.51	0.45	0.30	-
	30	0.69	0.56	0.50	0.45	0.40	0.28

This tendency is more evident with the increase of the channel slope and with the increase of the initial fluid depth in the reservoir. For instance, at the initial depth of 20 cm, and volume concentration of 27.4%, the wave front of the mixture propagates at a rate 0.34, 0.31 and 0.30 times the water wave velocity, if the channel slope is 0, 0.05 and 0.1%, respectively (Table 4). On the other hand, at the channel slope of 0.1%, and the concentration of 20.1%, the wave front of the mixture propagates at a rate 0.46, 0.45 and 0.45 times the water wave front velocity, if the initial depth is 10, 20, and 30 cm, respectively (Table 4).
At the maximum concentration (36.1%), some initial reservoir depths were not sufficient to set the mixture in motion (empty cells in Table 4). On the other hand, some hyperconcentrated mixtures

cease flowing after a certain distance x_o. This is the location of the wave front "freezing point". The relationship between distance x_o, channel slope and concentration, is given in Fig.9.

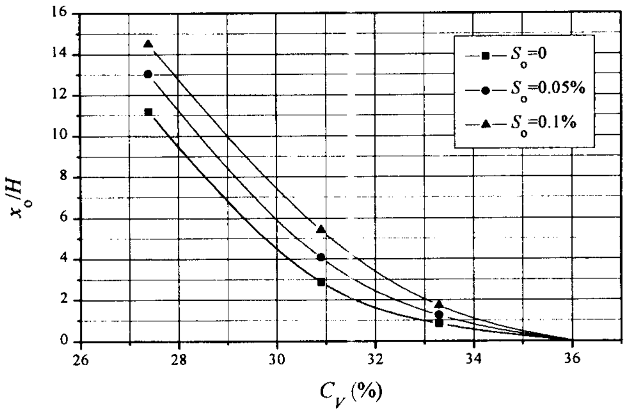

Fig. 9. Relationship between wave front travel distance, channel slope and concentration.

A typical diagram of the flow depth temporal variation is depicted in Fig.10 for the channel slope of 0.1%. The steepness of the wave front increases with concentration.

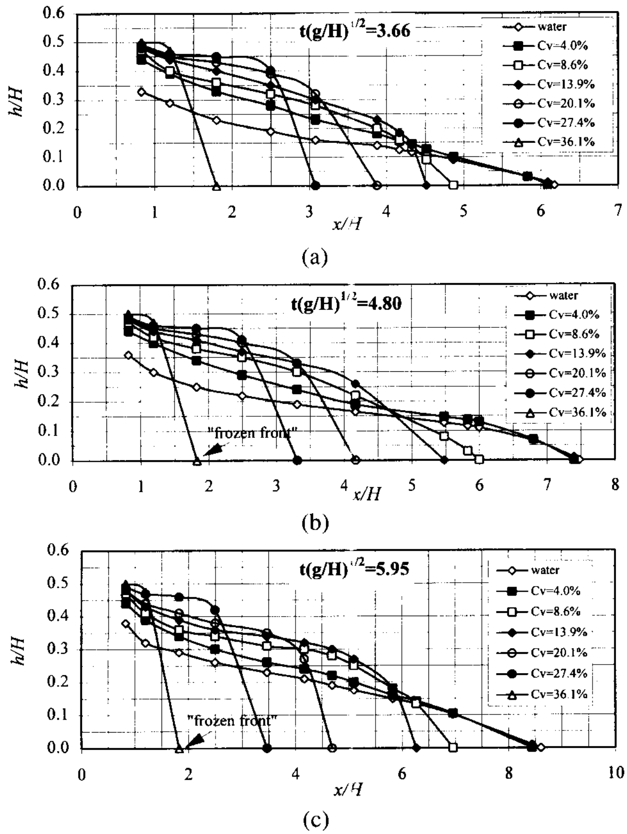

Fig. 10. The effects of concentration on flow depths.

The influence of particle concentration on the unsteady flow characteristics, can be also demonstrated by dimensionless stage hydrographs. The ones given in Fig.11 clearly show that the increase of concentration results in slower wave propagation, higher flow depths and a more pronounced increase of depth in the initial period.

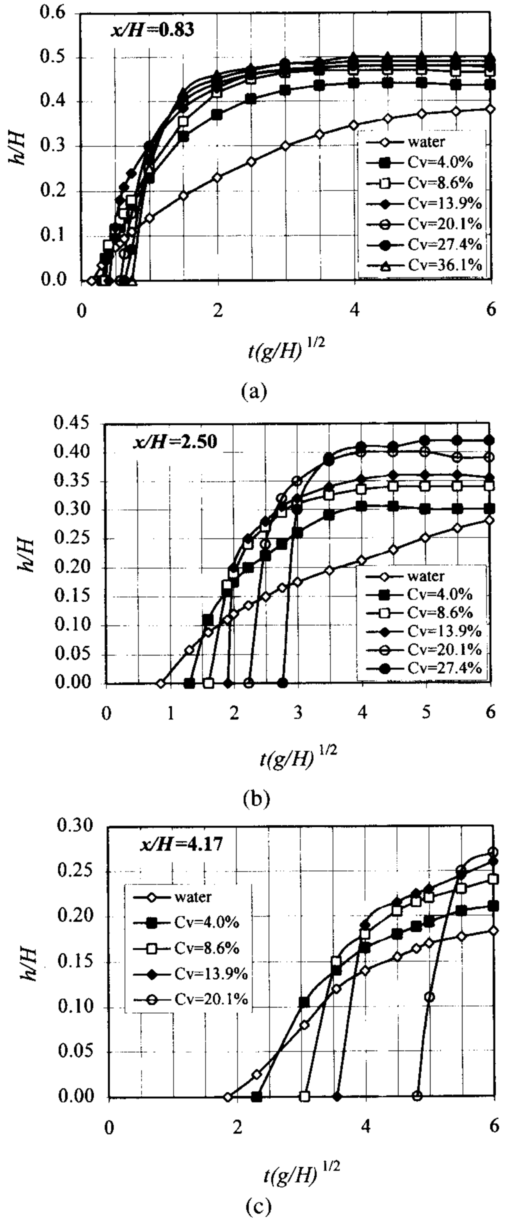

Fig. 11. Stage hydrographs at different cross-sections.

The analysis of flow depth dependence on concentration in terms of mixture depth to water depth ratio, is given in Table 5. As can be seen, the flow depth increases with concentration, while the ratio diminishes with time. The variation of mixture depth to water depth ratio along the channel is given in Table 6. A general increase of this ratio with distance is apparent.

Table 5. Ratio of mixture to water depth for $x/H = 2.5$ and $S_o = 0.1\%$.

Time	Volumetric concentration (%)					
$t\sqrt{g/H}$	4.0	8.6	13.9	20.1	27.4	36.1
2.50	1.47	1.80	1.87	1.60	-	-
3.66	1.49	1.67	1.74	1.97	2.00	-
4.80	1.20	1.36	1.44	1.60	1.68	-
5.95	1.07	1.21	1.27	1.39	1.50	-

Table 6. Ratio of mixture to water depth for $t\sqrt{g/H} = 5.95$ and $S_o = 0.1\%$.

Distance	Volumetric concentration (%)					
x/H	4.0	8.6	13.9	20.1	27.4	36.1
0.83	1.16	1.24	1.26	1.26	1.29	1.32
2.50	1.11	1.26	1.33	1.44	1.56	-
4.17	1.11	1.26	1.37	1.42	-	-
5.83	1.07	1.13	1.20	-	-	-

6 Conclusions

1. The water-clay mixtures exhibit non-Newtonian behaviour if the concentration of the solid phase is sufficiently high – for the analysed kaolinite clay suspensions, at the volumetric concentrations over about 10%. This conclusion is in accordance with findings reported in literature for other types of solid-liquid mixtures [1], [12].
2. The viscosity-concentration correlations, obtained by rotary viscometer measurements, indicate that the Bingham model can be used to describe such fluids. The dependence of the yield stress and the plastic viscosity on the clay particle concentration is given in Fig.2, and by equation (2).
3. Using the given rheological parameters, the water-clay laminar flow friction factors can be determined, either by calculating the Reynolds and Hedström numbers from equation (6) and using graphs in Fig.6, or by applying the extended Reynolds number concept, equation (8), and using the Moody-type diagram (Fig.7).
4. In the case of the dam-break type of unsteady flow, water-clay waves propagate generally at slower rates than water waves. The propagation velocity depends on concentration, the initial reservoir depth and the channel slope, as shown in Fig.8. At sufficiently high concentrations, the wave fronts "freeze" at certain distances, shortly after being set in motion (Fig.9).
5. The flow depths generally increase with concentration of solid particles and are higher than water depths (Figs.10–11). The ratio of mixture depth to water depth decreases in time in one given cross-section. At one given moment, this ratio tends to increase along the channel.

Notations

B channel width
C_v volumetric concentration of the solid phase
C_w solid phase concentration by weight
f Darcy-Weisbach friction factor
g acceleration due to gravity
h flow depth

H initial reservoir depth
He Hedström number
Q volumetric discharge
Re_1 Reynolds number
Re_2 extended Reynolds number
S_o channel bottom slope
t time
u local velocity
V mean cross-sectional velocity
x coordinate in the flow direction
x_o "freezing point" distance
y coordinate perpendicular to the flow direction
z vertical coordinate
$\dot{\gamma}$ rate of shear
η plastic viscosity
ρ_m mixture density
τ shear stress
τ_o bottom shear stress
τ_c yield stress

References

1. COUSSOT, Ph., Steady, laminar, flow of concentrated mud suspensions in open channel, Journal of Hydraulic Research, Vol. 32, No.4, 1994.
2. JOVANOVIĆ, M., KOMATINA, D., Experimental Study of a Non-Newtonian Flow, Journal of Theoretical and Applied Mechanics, Yugoslav Association of Theoretical and Applied Mechanics, No. 19, 1993.
3. KERESELIDZE, N.B., KUTAVAIA, V.I., Experimental Research on Kinematics of Flows With High Suspended Solids Concentration, Journal of Hydraulic Research, Vol. 33, No.1, 1995.
4. KOMATINA, D., Open-Channel Flow of Hyperconcentrated Mixtures, Master of science dissertation, Faculty of Civil Engineering, Belgrade, 1993 (in Serbian).
5. MIYAMOTO, K., EGASHIRA, S., MUD and Debris Flows, Journal of Hydroscience and Hydraulic Eng., special issues, Research and Practice of Hydraulic Eng. in Japan, No.SI-2: Fluvial Hydraulics, JSCE, 1993.
6. O'BRIEN, J.S., JULIEN, P.Y., Laboratory Analysis of Mud flow Properties, Journal of Hydraulic Engineering, ASCE,Vol. 114, Aug. 1988.
7. OGIHARA, Y., MIYAZAWA, N., A Proposal on Extended Reynolds Number, 21st IAHR Congress, Melbourne, Australia, 1985.
8. OGIHARA, Y., MIYAZAWA, N., Laws of Resistance of Pipe Flow of Solid-Liquid Mixtures, Journal of IAHR, Volume 29, No. 2, 1991.
9. QIAN, N., WAN, Z., A Critical Review of the Research on the Hyperconcentrated Flow in China, IRTCES, Beijing, China, 1986.
10. QIAN, Y., YANG, W., ZHAO, W., CHENG, X., ZHANG, L., Experimental Study on Homogeneous Hyperconcentrated Flow, Proc. of the International Workshop on Flow at Hyperconcentrations of Sediment, IRTCES, Beijing, China, 1985.
11. SKELLAND, A., Non-Newtonian Flow and Heat Transfer, John Wiley, New York, 1967.
12. SLOFF, C.J., Study on Modelling the Morphology of Torrents on Volcano Slopes, Journal of Hydraulic Research, Vol.31, No.3, 1993.
13. WAN, Z., WANG, Z., Hyperconcentrated flow, IAHR monograph series, Balkema, Rotterdam, 1994.
14. WANG, Z., LARSEN, P., XIANG, W., Rheological Properties of Sediment Suspensions and their Implications, Journal of Hydraulic Research, Vol.32, No. 4, 1994.
15. ZHANG, H., REN, Z., Discussion of Law of Resistance of Hyperconcentration Flow in Open Channel, Scientia Sinica, Ser.A, Vol. XXV, No.12, 1982.